

# Stripper foil considerations for PIP-II to Mu2e-II

David Neuffer<sup>a</sup>

<sup>a</sup>Fermilab, PO Box 500, Batavia IL 60510 USA

**Abstract.** The PIP-II linac produces 800 MeV  $H^-$  beam. The Mu2eII production target is immersed in a high B-field, which would strip  $H^-$  ions. Thus it is desired to strip the  $H^-$  ions before they reach the mu2e facility. We discuss design considerations for the stripper foil and its location, foil heating and related extinction design issues.

**Keywords:** muon, beams, PIP-II

## INTRODUCTION

The PIP-II project will provide a 800 MeV proton beam with cw capability, with beam power up to the MW level available for user experiments.[1] An upgraded or extended version of the Fermilab mu2e experiment[2 ,3], labeled mu2e-II, has been identified as a primary future user of that beam.[4] The mu2e experiment will initially use 8 GeV proton beam from a compact bunch stored in the Delivery Ring, extracted by slow extraction, and is limited in intensity to  $<10$  kW. The PIP-II beam could instead provide more than 100 kW of 800 MeV beam directly from the linac, where the linac beam can be formed into timing sequences that can match mu2e experimental requirements very precisely. The mu2e collaboration has expressed interest in an extension to the mu2e experiment based on the PIP-II linac. [5]

Our initial framework for mu2e-II is to begin with the mu2e Detector layout, but inserting 800MeV beam in place of the 8 GeV beam, and reusing as much of the initial experiment infrastructure as practical. Fig. 1 shows that detector, with the proton beam injection indicated by an arrow. The proton beam is injected off-center directed toward a production target in the production solenoid (PS). [6]

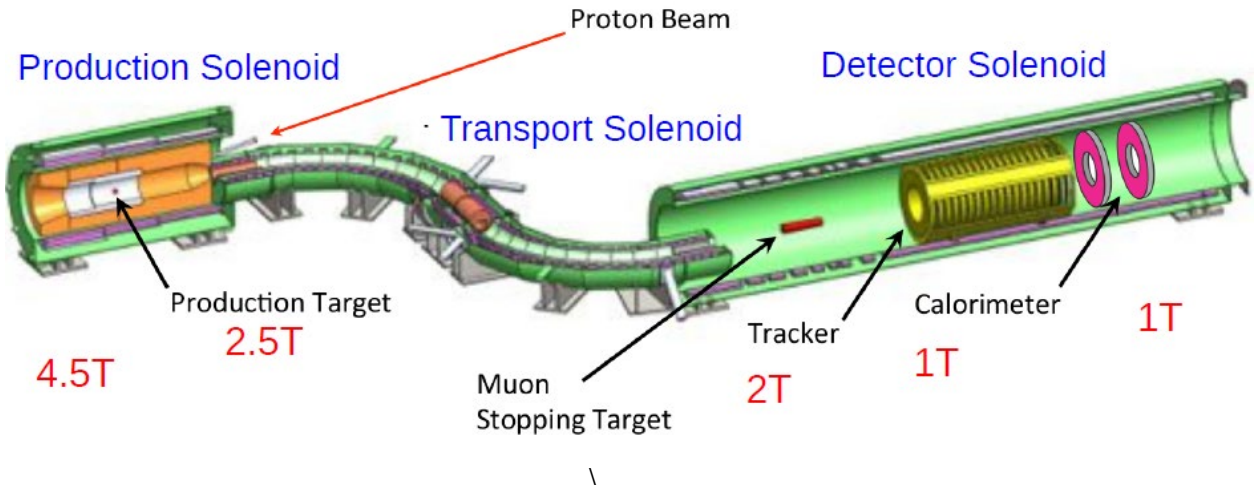


**FIGURE 1.** The mu2e Detector. Proton beam is injected off-axis toward the production target, producing secondaries that are transported to the Al stopping target.  $\mu \rightarrow e$  conversion events are detected as 105 MeV electrons in the tracker/calorimeter.

In the Mu2e-II extension, the 8 GeV p beam is replaced by the 800 MeV beam from PIP-II. However, the PIP-II beam is  $H^-$ . For compatibility with  $H^-$  injection into the Booster, the linac accelerates  $H^-$  ions, and the bending fields in the PIP-II transports are limited to 0.25T to avoid magnetic stripping to  $H^0$ .  $H^-$  ions would therefore be sent down

the mu2e-II line. However the production solenoid (PS) has fields up to ~4 T before the target. At an injection angle of 13.6°, this implies  $B_{\perp} \approx 0.9$  T perpendicular to the beam. The stripping time can be estimated using the formula of Schrek:

$$\tau = \frac{a}{3.197 B_t p} \exp\left(\frac{b}{3.197 B_t p}\right) \text{ seconds,}$$

where  $p = 1.463$  GeV/c for 800 MeV  $H^-$ ,  $B_t = 0.9$  T, and  $a$  and  $b$  are parameters fitted from data. [7, 8] Keating et al. obtained  $a = 3.073 \cdot 10^{-14}$  and  $b = 44.14$  from 800 MeV data. [9] At these parameters  $\tau = 2.62 \cdot 10^{-10}$  s or ( $c \tau = 8$  cm). Thus much of the  $H^-$  would strip to  $H^0$  within the magnet, and non-interacting  $H^-$  and  $H^0$  would strip to p ( $H^+$ ) in the target.

The mixture of charge states in the PS would make the beam transport to and past the target difficult to control. It would therefore be desirable to strip the linac  $H^-$  beam in the mu2e-II transport upstream of the production target so that only proton beam reaches the PS. This stripper should be downstream of the separation from the Booster line and possibly upstream of the bend into the mu2e line. (The bend would separate out unstripped  $H^-$  and  $H^0$ .) The stripper would be a thin carbon or diamond foil, similar to that used for  $H^-$  injection into the Booster or that used at SNS for 800 MeV  $H^-$  injection.

### Stripping Foil considerations

In the foil the  $H^-$  ions are stripped to  $H^0$  and  $H^+$ , and  $H^0$  ions are stripped to  $H^+$ . Equations for stripping versus foil thickness have been developed by Gulley et al., from fits to measured stripping data [10, 11]. The equations are:

$$f_{H^-}(t, \beta) = \text{Exp}[-(0.479 + 0.0085) \cdot 0.05t / \beta^2]$$

$$f_{H^0}(t, \beta) = \frac{0.479}{(0.479 + 0.0085 - 0.187)} \left( \text{Exp}[-(0.187) \cdot 0.05t / \beta^2] - \text{Exp}[-(0.479) \cdot 0.05t / \beta^2] \right)$$

$$f_{H^+}(t, \beta) = 1 - f_{H^0}(t, \beta) - f_{H^-}(t, \beta)$$

where  $\beta = v/c$  is the usual kinematic factor for the incident  $H^-$ ,  $t$  is the carbon foil thickness in  $\mu\text{gm}/\text{cm}^2$ . For a 500  $\mu\text{gm}/\text{cm}^2$  thick foil, 99.8% of initial  $H^-$  are stripped to  $H^+$  (protons). For graphite (at  $\rho = 2.0$   $\text{gm}/\text{cm}^3$ ), this is a 2.5  $\mu\text{m}$  thick foil, or 1.4  $\mu\text{m}$  thick for diamond ( $\rho = 3.6$ ). Figure 2 shows the variation of ion fraction through a foil with thickness of 500  $\mu\text{g}/\text{cm}^2$ .

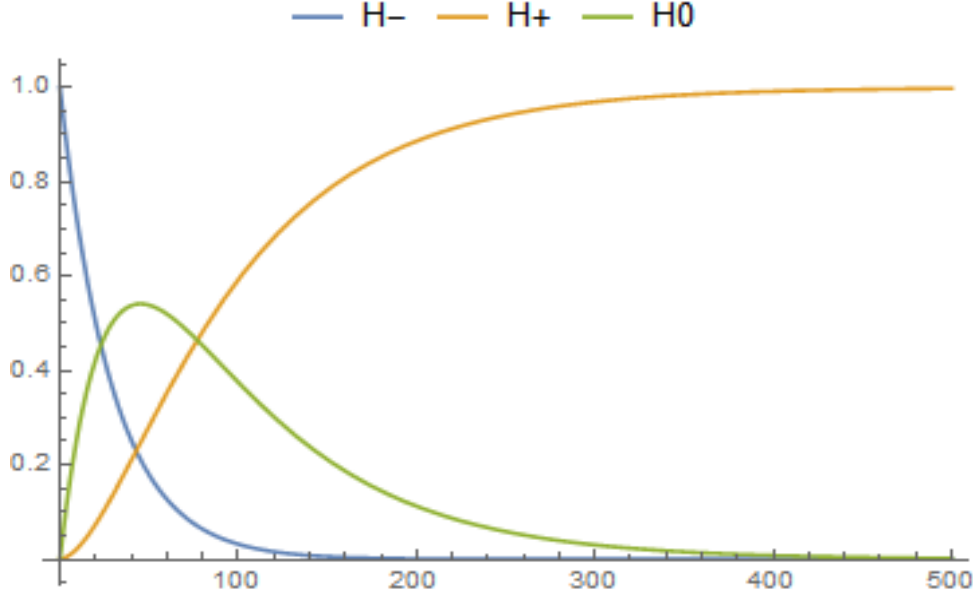


**FIGURE 2.** Fraction of beam that is  $H^-$ ,  $H^0$ , or  $H^+$  as it passes through a C foil with final thickness of  $500 \mu\text{g}/\text{cm}^2$ . At  $300 \mu\text{g}/\text{cm}^2$ , the beam is  $\sim 97\%$   $H^+$ , and  $3\%$   $H^0$ . At  $500 \mu\text{g}/\text{cm}^2$ , it is  $\sim 99.8\%$   $H^+$ . At  $400 \mu\text{g}/\text{cm}^2$ , it is  $\sim 99.2\%$   $H^+$ .

It is important that the multiple scattering caused by the foil be small compared to the emittance of the beam. The normalized emittance of the PIP-II  $H^-$  beam is  $0.3 \text{ mm-mrad}$ . The multiple scattering increase in the emittance is

given by:

$$\Delta\epsilon_N \cong \frac{\beta_T (13.6)^2 t}{2\beta^2 P_{\text{beam}} m_{\text{beam}} X_0}, \quad (1)$$

where  $P_{\text{beam}} = 1460 \text{ MeV}/c$ ,  $m_{\text{beam}} = 938 \text{ MeV}/c$ , and  $X_0 = 42.7 \text{ gm}/\text{cm}^2$ , the radiation length for carbon (C). For  $t = 0.0004 \text{ gm}/\text{cm}^2$  and a focusing betatron function of  $\beta_T$  of  $10\text{m}$ , we obtain  $\Delta\epsilon_N = \sim 0.009 \text{ mm-mrad}$ . This is adequately small. However a much larger  $\beta_T$  ( $\beta_x$  or  $\beta_y$ ) at the absorber could lead to unacceptable increase.

Energy loss for protons in graphite is  $\sim 4.5 \text{ MeV}/\text{cm}$  or  $\sim 0.9 \text{ keV}$  in the  $2\mu\text{m}$  foil; this is  $\sim 10^{-6}$ . Increase in energy spread is an order of magnitude smaller. The beam is relatively unaffected by the single passage through the foil, except for the change in charge, and optics

## Beam Transport and stripper location

Fig. 2 displays the PIP-II linac as it will be constructed on the Fermilab site, with the  $800 \text{ MeV } H^-$  beamlines to the Booster and mu2e indicated. A. Vivoli designed beamline lattices for this geometry [6]. The lattices do not contain  $H^- \rightarrow H^+$  stripping, so must be modified to include this. Fig. 3 shows betatron functions for the line. A possible location for a stripper foil would be somewhere after the bend that separates the mu2e beam line from the Booster injection line but before the bend toward the mu2e experimental hall.

In this section the Vivoli lattice has a coupled horizontal and vertical dispersion wave. A particularly desirable foil location could be half-way through this section where both dispersions pass through zero (at  $z=257.5 \text{ m}$  from the start). At that point  $\beta_x = 3.4 \text{ m}$  and  $\beta_y = 15.3 \text{ m}$  ( $\sigma_x = 0.8\text{mm}$ ,  $\sigma_y = 1.52\text{mm}$ ), which would imply a fairly small beam spot on the foil. The incident energy loss power at the beam spot would be  $31 \text{ kW}/\text{m}^2$  ( $\sim 0.3 \text{ W}$  total ...), where this estimate includes energy loss from the proton and the two stripped electrons.

This density could be reduced by a larger beam spot. If  $\beta_x$  and  $\beta_y$  were increased to  $30\text{m}$ , the energy density would be reduced to  $\sim 7 \text{ kW}/\text{m}^2$ , and the multiple scattering increase in emittance would still be less than  $\sim 10\%$ .

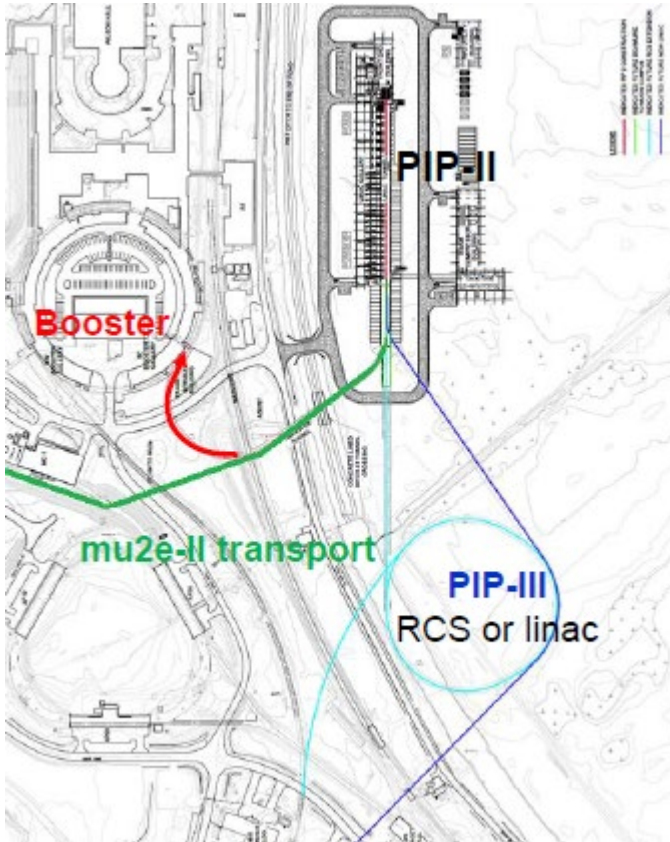


**Figure 2.** PIP-II linac with transport lines to Booster (red) and mu2e-II (green) indicated.

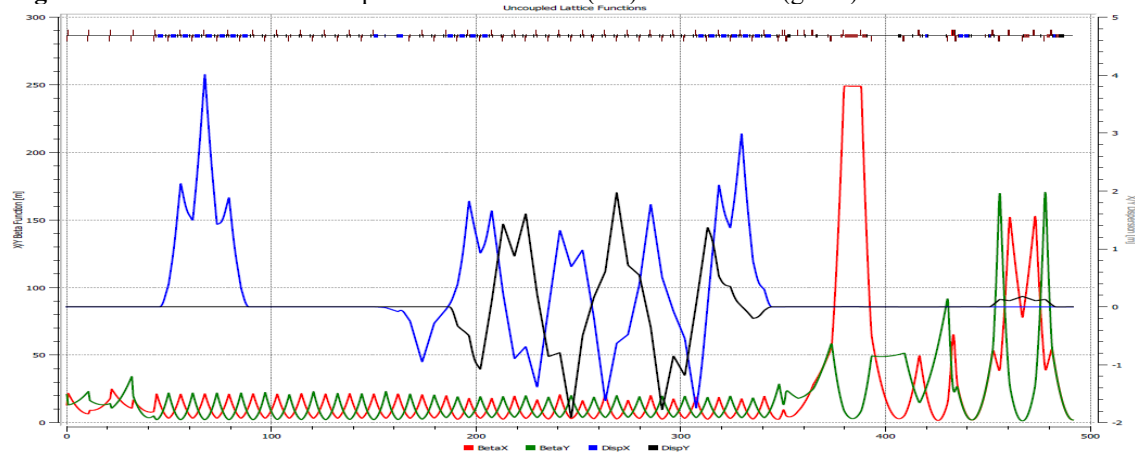


**Figure 3.** Betatron functions along the beamline to mu2e-II.

### Foil heating estimates

The beam stripping would heat the foil, and foil heating has been a significant problem in foils for multi-turn stripping injection in synchrotrons. These problems should be significantly less for the PIP-II to mu2e line since beam particles pass through only once, and the beam is nearly cw. (Pulsed injection concentrates energy heating in short pulses, leading to temperature spikes much higher than equilibrium.)

The temperature heating can be estimated using equations presented by Liaw et al. and Drozhdin et al. In the approximation of only radiative cooling, the evolution of temperature at the center of the incident beam (defined by the central density  $1/(2\pi\sigma_x\sigma_y) = 1/A$ ).

$$\rho V C_h \frac{dT}{dt} \cong \frac{dE_{H \rightarrow p}}{ds} t \frac{I}{e} - 2A\epsilon\sigma_B(T^4 - T_0^4) \quad (2)$$

where  $T(t)$  is the temperature,  $\rho$  is the density,  $C_h$  is the heat capacity, which is a function of temperature for graphite,  $t$  is the foil thickness,  $V=At$  is the sample volume,  $dE/ds$  is the energy loss (which includes contributions from the proton and electrons),  $I/e$  is the beam current,  $\epsilon$  is the efficiency (0.8 for graphite),  $\sigma_B$  is Boltzmann's constant,  $T_0$  is the background temperature (297° K). After inserting some numbers associated with mu2e-II,  $I=0.0001$  A,  $t=0.000002$   $\mu$  (400  $\mu\text{g}/\text{cm}^2$ ),  $dE/ds = \sim 7$  MeV/cm,  $\rho = 2$  gm/cm,  $C_h \cong 12 + 2.87 T - 0.00145 T^2 + 3.1 \cdot 10^{-7} T^3 - 2.4 \cdot 10^{-11} T^4$  J/kg/°K,  $\sigma_B = 5.67 \cdot 10^{-8}$  W/m<sup>2</sup>K<sup>4</sup>, we find a dependence of  $T$  with time given by fig. 4. The foil hot spot increases to  $\sim 760$  °K within a fraction of a second.

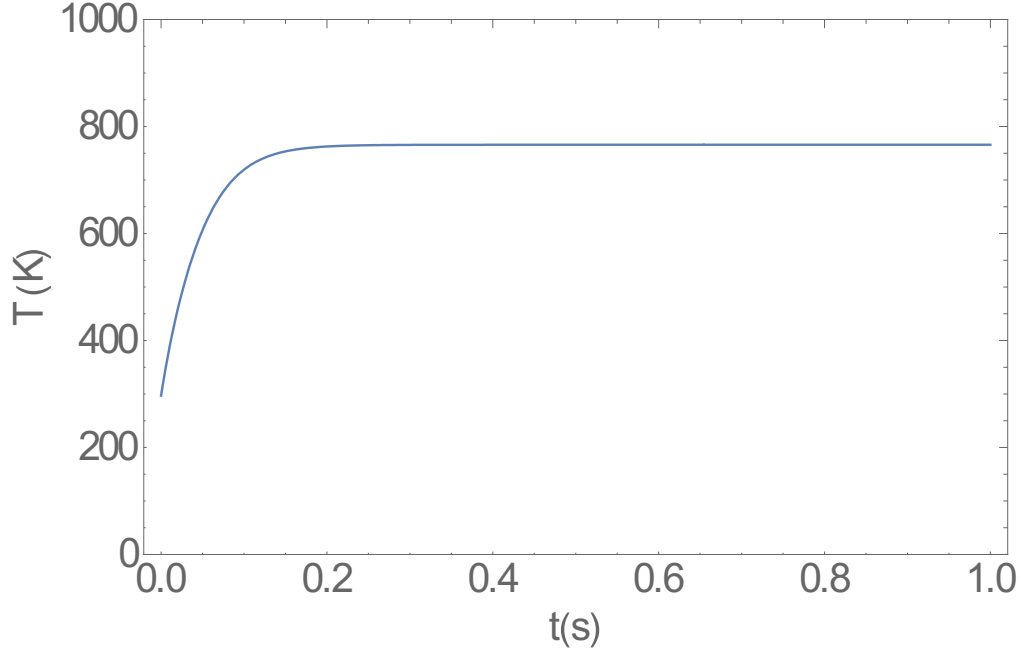


**Figure 4.** Foil temperature development over 1s, with beam starting at  $t=0$ .

The peak temperature could be reduced by increasing the spot size at the foil. For example, with  $\beta_x, \beta_y$  set to 30m ( $\sigma = 2.5\text{mm}$ ), the peak temperature is reduced to  $\sim 540$  °K.

The temperature behaviour is much milder than that in other foil situations, particularly those with pulsed beam. In ref. 12, the stripper foil temperature at SNS spikes to  $\sim 1800$  °K at the 60 Hz pulse frequency, with an equilibrium of  $\sim 1000$  °K. (Incident beam power is much larger at SNS.) Foil damage should be a much smaller risk in the mu2e-II facility.

If the 100 kW is increased to 1MW in the PIP-II beam line, the equilibrium temperature increases to  $\sim 1350$ °K in the initial lattice, and to 940 °K in the 2.5mm beam spot examples. Thus, higher power PIP-II applications will need a more careful calculation of temperature effects and some mitigation development.

The simplified model of eq. (2) does not include conduction and other effects; also the temperature distribution across the foil is not calculated. In practice, the hot spot should be moved around the foil (or the foil moved) to minimize localized foil distortion. A particularly desirable configuration would be a rotating foil, such as that used by Hasabe et al. for U stripping[14] at RIKEN and was also studied for the Proton Driver by Johnson and Tang.[15] These variations would be needed if a higher power PIP-II beam (MW-scale) was using stripping foils.

## Extinction Considerations

The mu2e-II experiment requires an extinction level of better than  $10^{-12}$ , which means the incoming beam intensity during the beam-free portion of the experiment time cycle must be less than  $10^{-12}$  of the beam intensity during the beam injection portion. (The beam injection is within  $\sim \pm 125$  ns from  $t=0$  of the  $\sim 1695$  ns cycle for Mu2e.)

For mu2e-II the primary extinction occurs at the PIP-II source, which is designed to be able to include or exclude beam in each of the 162.5 MHz rf buckets of the PIP-II beam source. A typical injection might include beam in a sequence of  $\sim 8$  buckets (out of  $\sim 275$  in a 1693 ns cycle) with beam excluded from the following  $\sim 267$  buckets. The degree of accidental injection into these buckets is not precisely known, but is expected to be better than  $\sim 10^{-5}$ . An experiment at the PIP2IT prototype of the PIP-II source will provide a more accurate value for this. (The buckets closest to the injection sequence are expected to have relatively less extinction. The high-extinction window would not include these.)

A secondary extinction system is expected to be necessary to reach the  $10^{-12}$  level. T. Roberts has suggested that bumping the beam off the stripper foil in the extinction window would leave stray beam in that window unstripped and therefore removed by downstream dipoles and collimation.[16] It is not clear that this could obtain the full desired extinction. Future design studies and simulations could determine this. It would, at least, provide an additional extinction cut for the experiment.

The Mu2e experiment has a secondary extinction system that consists of an AC dipole that is designed to deflect out of time beam onto collimators, and, together with the  $\sim 10^{-4}$  extinction associated with the proton beam rf bucket, provide  $\sim 10^{-11}$  extinction. The same system could also be used for Mu2e-II with minor modifications. The last section of the transport section from PIP-II (see fig. 3) uses the same elements of final focus transport used for Mu2e and includes the elements of the Mu2e extinction system. The AC dipole would be located at the high- $\beta$  region at  $z = 390$  m ( $\beta_x = 250$  m). the associated collimators are located at  $z=430$  m. The system could work with little modification because the beam sizes of the Mu2e 8 GeV proton beam and the 800 MeV Mu2e-II beam are similar. While the transverse normalized rms emittances differ ( $\sim 2.5$  mm-mrad at 8 GeV and 0.3 mm-mrad at 800 MeV, the unnormalized emittances are similar ( $\sim 0.26$  mm-mrad for Mu2e and  $\sim 0.2$  mm-mrad for mu2e-II) With magnet fields at  $\sim 1/6$  value to match the lower momentum, the 800 MeV and 8 GeV beams have the same optical functions and thus similar beam sizes.

The AC dipole wave form consists of two harmonics, with strengths designed to give a flat region with very little deflection for the center of the injection window and to give very large deflections outside the injection window. The wave form is shown in eq. 4:

$$Kick \propto A \left( \sin\left(\frac{\pi t}{T_0}\right) - f \sin\left(\frac{h\pi t}{T_0}\right) \right) \quad (4)$$

where  $A$  is the kick amplitude,  $T_0$  is the cycle period (1.695 ns)  $h$  is the (odd integer) harmonic number and  $f$  is the relative strength of that harmonic. For Mu2e,  $h = 15$ ,  $f=0.084$ . This gives an injection window with full width of 250 ns. Fig. 5 shows the amplitude of the kick in the injection window.

Use of that at  $1/6$  strength would give the same angular deflections (and same secondary extinction) for mu2e-II. The mu2e-II injection beam length is much shorter and a shorter injection window would be preferred. this can be obtained by changing the AC Dipole kick parameters. Fig. 5 shows the result of using  $A = 2.5/6$ ,  $h=21$ ,  $f=0.055$ ; this obtains an injection full-width of  $\sim 125$  ns with extinction outside that window.

The combination of injection and secondary extinction should be adequate for Mu2e-II.

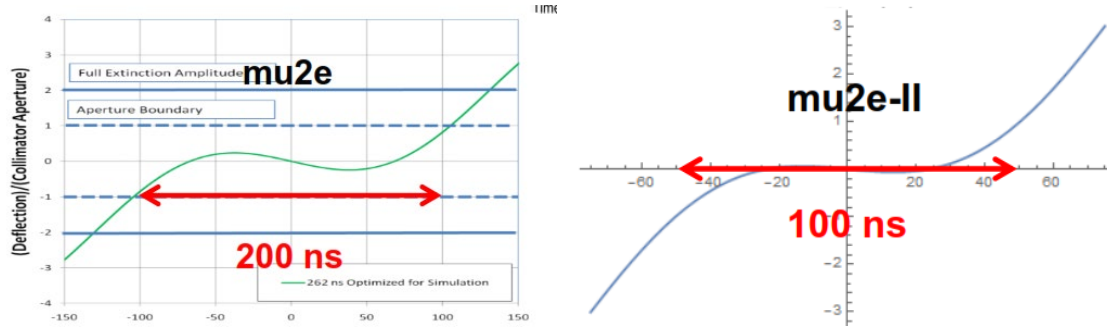


**Figure 5.** (Left) AC Dipole kick over the injection window with the Mu2e injection width. (Right) AC dipole kick matched to the shorter Mu2e-II injection width. In both cases, a kick with magnitude greater than 2 removes the beam from the transport.

## ACKNOWLEDGMENTS

We thank D. Glenszinski and J. Miller for encouraging comments. This research is supported by Fermi Research Alliance, LLC under Contract No. DE-AC02-07CH11359 with the U.S. Department of Energy, Office of Science, Office of High Energy Physics.

## REFERENCES

1. M. Ball et al., The PIP-II Conceptual Design Report (2017).
2. Bartoszek, L. et al., Mu2e Technical Design Report, Mu2e Doc 4299, arXiv 1501.0524.(2015).
3. Mu2e Conceptual Design Report, Mu2e Document 1169-v12 (2012).
4. K. Knoepfel et al., “Feasibility Study for a Next-Generation Mu2e Experiment”, arXiv:1307.1168v2 (2013).
5. F. Abusalma et al., “Expression of Interest for Evolution of the Mu2e Experiment”, Mu2e docdb-10655, Feb. 18, 2018.
6. D. Neuffer, “Mu2e-II Injection from PIP-II”, Fermilab TM-2677-AD-APC, April, 2018.
7. W. Chou et al., “8 GeV H<sup>-</sup> ions: transport and injection,” Proc. PAC 2005, Knoxville, TE, p. 1222 (2005).
8. L.R. Scherk, Canadian J. of Phys, 57, 558 (1979).
9. P.B. Keating et al., Phys. Rev. A 52, 4547 (1995).
10. M. S. Gulley et al., *Physical Review A* 53, 3201-3210 (1996).
11. M. Plum, “Stripper Foils for H<sup>-</sup> Beams”, in Handbook of Accelerator Physics and Engineering, second edition, A. W. Chou, K. H. Weiss, Tigner and F. Zimmermann, eds., p. 574 (2013).
12. C. J. Liaw et al., Proc PAC 1999, New York, NY, p. 3300 (1999).
13. A. I. Drozhdin, I. L. Rakhno, S. I. Striganov, and L. G. Vorobiev, Phys. Rev. STAB 15, 011002 (2012).
14. H. Hasebe et al., “Development of a rotating graphite carbon disk stripper” AIP Conf. Proc. **1962**, 030004 (2018).
15. D. Johnson and Z. Tang, “Rotating Foil and Stripping Station Studies”, unpublished (2012).
16. T. Roberts, unpublished (2015).